



Development and Performance Study of Mutually Coupled Parasitically Loaded 5G Antenna for Sub-6GHz Applications

Sudharani Chidurala¹ · Prakasa Rao Amara¹

Received: 29 May 2024 / Revised: 29 May 2024 / Accepted: 17 June 2024

© The Author(s), under exclusive licence to Springer Science+Business Media, LLC, part of Springer Nature 2024

Abstract

The edge-fed monopole 5G antenna described in this article is intended for sub-6 GHz applications, with a specific focus on the n77 (3.7 GHz), n78 (3.5 GHz), and n79 (4.5 GHz) frequency bands. A novel methodology is employed to develop the antenna, which consists of binary operations on three patches (Patch1, Patch2, and Patch3), with their dimensions optimized for 3.5 GHz, 3.7 GHz, and 4.5 GHz, respectively. In order to generate an initial U-stub, Patch2 is subtracted from Patch1 followed by Patch3. Through the utilization of a coupling limb, Patch3 and the U-stub establish mutual current coupling. To remove extra bandwidth and maintain a gain more than 5 dBi, the antenna is parasitically loaded with a splitting resonator (SRR) in a partial ground plane. The resultant antenna functions within the frequency range of 3.13 GHz to 5.06 GHz, exhibiting a maximum gain of 5.71 dBi and a maximum efficiency of 99.55%. By reducing its dimensions by 12.676% in comparison to a traditional rectangular patch antenna operating at 3.5 GHz ($0.416\lambda_0 \times 0.423\lambda_0 \times 0.0186\lambda_0$), the overall dimensions are as follows: $0.416\lambda_0 \times 0.369\lambda_0 \times 0.0186\lambda_0$. It is worth noting that λ_0 is computed at 3.5 GHz. The RLC equivalent circuit is validated using ADS software, and antenna prototype measurements accord with simulated outcomes generated by HFSS and CST software.

Keywords 5G · FR1 frequency range · Miniaturization · Mutual coupling · Parasitic loading · SRR · U-shape stub · Sub-6 GHz

✉ Sudharani Chidurala
sudha.ch2207@gmail.com

¹ Department of Electronics and Communication Engineering, National Institute of Technology, Warangal, India

1 Introduction

In the present time, 5G and 6G emerging technologies demand 5G antennas for numerous applications. The 5G bands are divided into sub-6 GHz and high-frequency millimeter (mm) waves. The lower frequencies are named as FR1(450 MHz to 7.275 GHz) while the higher frequencies mm-waves known as FR2 (> 24 GHz) [1, 2]. In the initial stage of 5G sub-6 GHz, 3.3–3.4 GHz, 3.4–3.6 GHz, and 4.8–5 GHz are deployed and the 3.3–3.6 GHz band becomes popular among all and named as n78-band. Chen et al. have proposed and investigated a compact Γ -shaped base station antenna for a 5G n78-band [2]. Varshney et al., have proposed a transformer-fed miniaturized antenna with a high radiation efficiency of 95.37% with a lower gain of 2.92 dBi. It is specifically suitable for sub-6 GHz n78 band [1]. Further, an enhanced patch size antenna with a frequency reconfigurable action antenna was proposed for wide-range coverage of wireless applications along with lower applications. Consequently, these yields interferences with other applications. The lower gain and limited bandwidth of this antenna limits its applications [3–5]. The enhanced patch size of the antenna makes these antennas constrained to use for 5G applications. Hence these 5G antennae require band eliminations to minimize interferences [5]. For use in the higher frequency band, it is necessary to miniaturize the size of the antenna [1, 6]. The gain of the antenna maintained above 5 dBi by converting single element miniaturized 5G antenna into multiple input multiple output antennas (MIMO) [6, 7]. There are several methods available to maintain the bandwidth of the antenna like introduction of slots, parasitic loading with metamaterials, split ring resonator (SRR) triplets, complementary split ring resonators (CSRR), stub loading, frequency selective surface and multi-layered antennas [3, 5, 6, 8, 9]. The reduction of antenna size is possible without a miniaturizing process is that to design any antenna at a higher frequency and then transform their performance parameters to use at lower frequencies [10]. Most of the antennas are designed specifically for n78 applications in 5G sub-6 GHz FR1 bands [1, 2, 6, 11]. Since the design of metamaterial to work as SRR. It is essential to design an SRR for maintaining antenna gain as well as to control the bandwidth. The SRR performance parameters (effective permittivity, permeability, and refractive index) are estimated using standard equations [8, 9, 12, 13].

Designing base station antennas that cover all three bands while maintaining optimal performance is challenging because to the requirement for a voltage standing wave ratio (VSWR) of less than 1.5 ($S_{11} < -14$ dB). Therefore, broadening impedance bandwidth is imperative. The wider bandwidth results in a lowering of the antenna gain [2, 6, 11, 14], and a higher gain results in the narrow bandwidth [1, 7]. Therefore, it is a challenging task to cover all the popular (n77, n78, and n79) 5G sub-6 GHz bands and reject other bands. Maintaining the antenna, gain above 5 dBi while controlling bandwidth is another big task in this 5G area. Most available literature antennas are available to cover only n78 bands.

The main bands of the lower frequency range 5G communication are n77(3.3–4.2 GHz), n78(3.2–3.8 GHz), and n79(4.4–5.0 GHz) bands. This research is primarily concerned with the coverage of three bands. Therefore, the antenna must have a lower frequency at 3.2 GHz and an upper frequency at 5.0 GHz. Therefore, the following are the main objectives of the proposed work;

- To design a Sub-6 GHz antenna in a lower FR-1 frequency range (1 GHz to 6 GHz) of 5G communications to cover n77, n78, and n79 bands with bandwidth from 2 to 5 GHz.
- The primary objective of this research is to investigate the parasitic loading impact of stubs and develop metamaterial designs. This work attempts to enhance the performance of the antenna by utilizing mutual coupling and parasitic loading of SRR and U-stubs to increase parameters such as gain, bandwidth, impedance matching, and radiation characteristics.
- This manuscript describes the development of a 5G antenna designed to operate within the frequency range of 3.2 GHz to 5.0 GHz. The antenna is intended to support the primary 5G frequency bands known as n77, n78, and n79. The antenna's bandwidth ranges from 3.13 GHz to 5.06 GHz, making it appropriate for these frequency bands. The design procedure entails use HFSS and CST software to create the antenna construction and incorporate a metamaterial Split Ring Resonator (SRR) to ensure a gain of at least 5 dBi and regulate the bandwidth within the FR-1 sweep.

The research is organized in the following manner:

1. Section 2: Describes the design and development of the microstrip edge-fed antenna structure. It covers the design of the metamaterial SRR, the impact of parasitic loading caused by a U-stub, adjustments to the patch, and the consequences of parasitic loading on the ground structure with SRR.
2. Section 3: Focuses on the fabrication of the designed antenna and its performance parameters detailed analysis and validation. It also explains the RLC equivalent circuit derived from the simulated design and verifies it using ADS software. Additionally, this section compares the performance parameters of the proposed antenna with similar existing recently published antennas.
3. Section 4: Concludes the proposed antenna's features, limitations, applications, and prospects.

This organization provides a comprehensive overview of the antenna design, fabrication process, performance analysis, and comparison with existing antennas. It emphasizes the distinctive attributes and contributions of the proposed antenna while exploring its possible applications and avenues for future investigation.

2 Material and Methods

2.1 Antenna Design

The proposed Sub-6 GHz antenna is developed on FR-4 Material of thickness 1.6 mm at a design frequency of $f_0 = 3.5$ GHz. The used FR4 substrate is lossy with loss tangent ($\tan\delta$) 0.02.

2.2 Design Equations

Basic general rectangular patch antenna (RPA) design Eqs. (1–11) are used to evaluate the patch dimensions at 3.5 GHz (patch 1), 3.7 GHz (patch 1), and 4.5 GHz (patch 1) [15–18].

Step 1: The width of the patch antenna is given by the equation:

$$W_P = \frac{C}{2f_0} \sqrt{\frac{2}{\epsilon_r + 1}} \quad (1)$$

where:

c: velocity of light is 3×10^8 m/s,

ϵ_r : Dielectric constant of the substrate.

f_0 : design frequency of antenna.

Step 2: Effective Dielectric constant of the RPA is determined as:

$$\epsilon_{\text{reff}} = \frac{\epsilon_r + 1}{2} + \frac{\epsilon_r - 1}{2} \left[\frac{1}{\sqrt{1 + \frac{2h}{W_P}}} \right] \quad (2)$$

Step 3: The effective length is at the design frequency:

$$L_{\text{eff}} = \frac{C}{2f_0 \sqrt{\epsilon_{\text{eff}}}} \quad (3)$$

Step 4: Extension length of the RPA computed with this equation:

$$\Delta L = 0.412h \frac{(\epsilon_{\text{eff}+0.3}) \left(\frac{W_P}{h} + 0.264 \right)}{(\epsilon_{\text{eff}-0.258}) \left(\frac{W_P}{h} + 0.8 \right)} \quad (4)$$

The length "L" of the PRA is calculated as:

$$L_P = L_{\text{eff}} - 2\Delta L \quad (5)$$

Step5: Radiation box Calculation:

$$\lambda = \frac{c}{f_0} \quad (6)$$

$$\lambda_g = \frac{\lambda}{\sqrt{\epsilon_{\text{reff}}}} \quad (7)$$

where,

$$\epsilon_{\text{eff}} = \frac{\epsilon_r + 1}{2} + \frac{\epsilon_r - 1}{2} \left[\frac{1}{\sqrt{1 + \frac{2h}{w}}} \right] \quad (8)$$

Step6: Feed calculations:

$$\text{Feed length, } L_F = \frac{\lambda_g}{4} \quad (9)$$

Step7: Width and Length of the substrate:

$$\text{Substrate width, } W_S = 3h + W_p + 3h \quad (10)$$

$$\text{Substrate length, } L_S = L_F + L_p + 3h \quad (11)$$

The proposed edge-fed monopole antenna consists of a patch designed at 4.5 GHz, U-stubs generated from the binary subtraction of the patches that are designed at 3.5 GHz and 3.7 GHz respectively, and a coupling arm in the main radiating patch as shown in the front view of Fig. 1a. The bottom of the antenna consists of a reduced ground whose length (L_G) is less than $\frac{\lambda_g}{4}$, and width (L_G) is equal to the substrate width that is parasitically loaded with the metamaterial single unit SRR as illustrated in Fig. 1b. The antenna patch structure is designed using a novel binary operation method to achieve the desired bandwidth below -10 dB. The trimetric view of the proposed antenna structure is shown in Fig. 1c. The dimensions parameters of the antenna are marked in Fig. 2a, b and their values are showcased in Table 1.

2.3 Antenna Design Development

The antenna structure is developed through seven steps, each illustrated in Fig. 3 with the front view of the patch and the bottom view of the ground.

1. Step 1: Initial Design

- The antenna patch is designed for 3.5 GHz with the entire bottom surface as ground.
- This configuration yields a narrow bandwidth from 5.14 GHz to 5.26 GHz.

2. Step 2: Ground Reduction

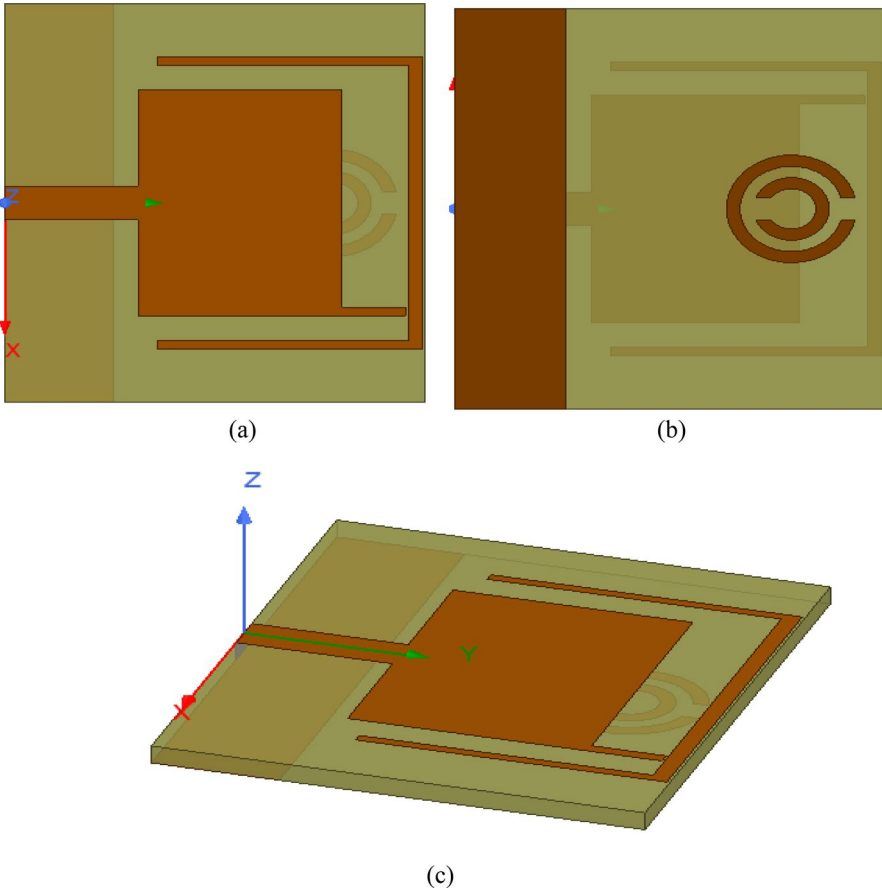


Fig. 1 Antenna Structure **a** front view, **b** rear view, and **c** trimetric view

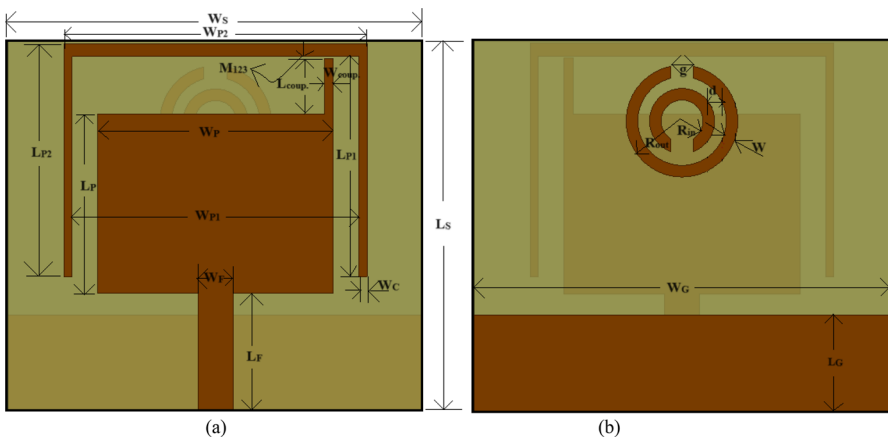


Fig. 2 Antenna dimensions parameters **a** top patch, and **b** bottom ground

Table 1 Dimensions of the proposed antenna

Parameter	Dimension (in mm)	Parameter	Dimension (in mm)	Frequency (GHz)
W_S	35.686	L_S	31.688	
W_F	3.0	L_F	10.037	
W_P	20.286	L_P	15.38	4.5 (Inner Patch)
W_{P1}	24.67	L_{P1}	18.87	3.7(Middle Patch)
W_{P2}	26.082	L_{P2}	19.988	3.5 (Outer Patch)
W_{coup}	0.8	L_{Coup}	4.8	
W_C	0.706	M_{123}	0.153	
W_G	35.686	L_G	8.2	
R_{in}	1.797	R_{out}	4.797	
g	2.0	d	1.0	
W	1.0	h	1.6	

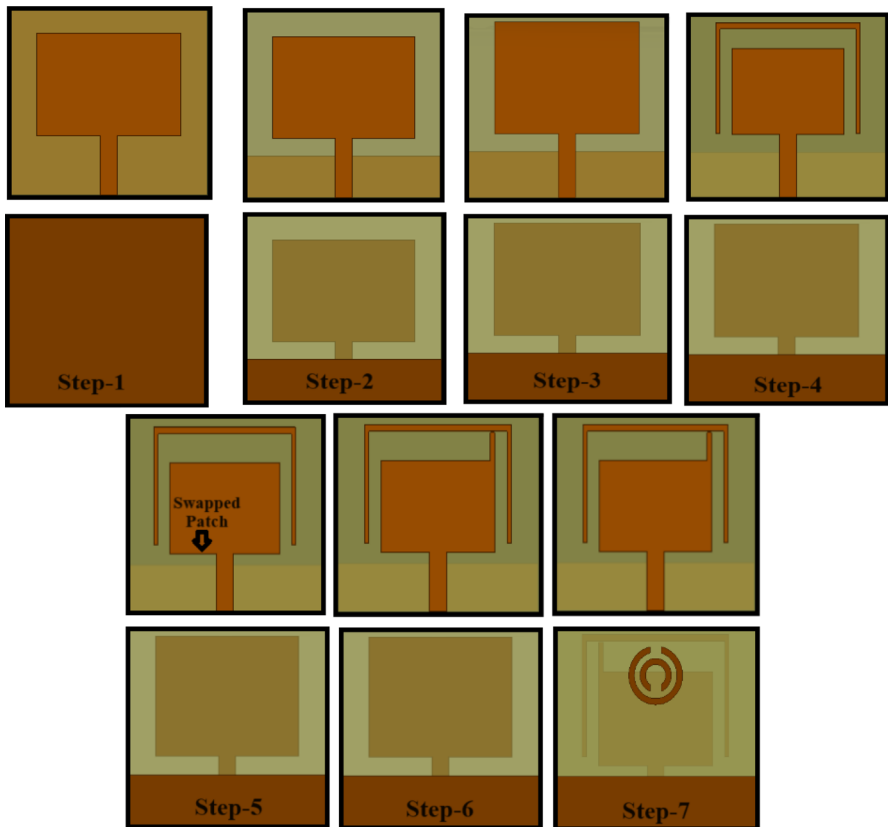


Fig. 3 Step by step Antenna structure development

- To create a wideband antenna, the ground plane is reduced towards the feed.
- This step broadens the bandwidth but increases reflection losses.

3. Step 3: Substrate Length Reduction

- The substrate length is reduced, which further increases reflection but miniaturizes the antenna to 12.676% of its original size.

4. Step 4: Patch Modification

- Without altering the reduced substrate size, a 3.7 GHz rectangular patch is subtracted from the 3.5 GHz patch, creating a U-stub.
- Additionally, a 4.5 GHz rectangular patch is attached to the feed, improving the reflection coefficient below -10 dB and widening the bandwidth, although antenna gain decreases.

5. Step 5: Patch Position Adjustment

- To further improve the reflection coefficient and bandwidth, the 4.5 GHz patch is moved closer to the port.
- This step results in a further reduction in gain.

6. Step 6: Mutual Coupling Arm Addition

- A mutual coupling arm is attached between the patch and the U-shaped stub.
- This modification enhances both the gain and the bandwidth of the antenna.

7. Step 7: Metamaterial Loading

- A single unit metamaterial Split Ring Resonator (SRR) is added to the ground.
- This eliminates the extra bandwidth below -10 dB and maintains the antenna gain above 5 dBi.

The step-by-step development of the antenna is summarized in Table 2.

Table 2 Step-by-step antenna structure development

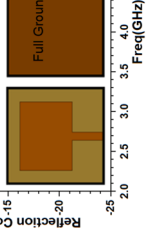

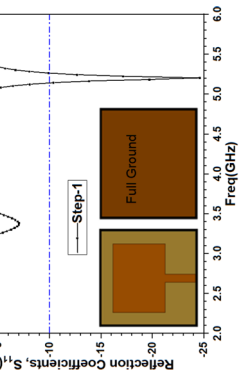


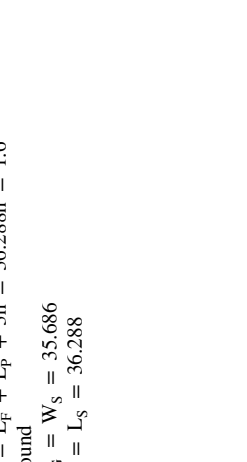
Step and antenna size (mm)	Patch (Front View)	Ground (Rear View)	Reflection Coefficient Characteristics (S_{11} Plot)	Antenna parameters
<p>Step-1</p> <p>$W_S = 3h + W_P + 3h = 35.686$ $L_S = L_F + L_P + 3h = 36.288h = 1.6$ Ground $W_G = W_S = 35.686$ $L_G = L_S = 36.288$</p>	<p>Patch1 at 3.5 GHz</p> 	<p>Full Ground</p> 		<p>Res. Freq $f_r = 5.2$ GHz BW (GHz) (5.14–5.26) Unidirectional Radiation Pattern Gain at 3.5 GHz is 6.06 dBi</p>
<p>Step-2</p> <p>$W_S = 3h + W_P + 3h = 35.686$ $L_S = L_F + L_P + 3h = 36.288h = 1.6$ Ground $W_G = W_S = 35.686$ $L_G = L_S = 8.2$</p>	<p>Patch1 at 3.5 GHz</p> 	<p>Reduced Ground</p> 		<p>Res. Freq $f_r = 3.72$ GHz BW (GHz) (3.36–4.01) Bidirectional Radiation Pattern Gain at 3.5 GHz is 4.86 dBi (Monopole antenna)</p>

Table 2 (continued)

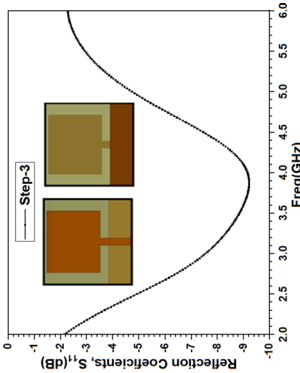
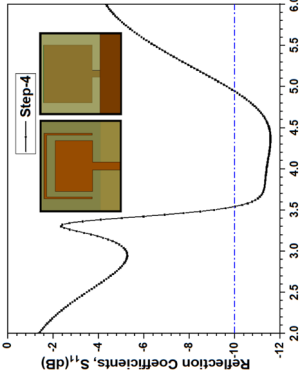
Step and antenna size (mm)	Patch (Front View)	Ground (Rear View)	Reflection Coefficient Characteristics (S_{11} Plot)	Antenna parameters
<p>Step-3</p> <p>$W_S = 3h + W_P + 3h = 35.686$</p> <p>$L_S = L_F + L_P + h - 1.4 = 31.688$</p> <p>$h = 1.6$</p> <p>Ground</p> <p>$W_G = W_S = 35.686$</p> <p>$L_G = L_S = 8.2$</p>	<p>Patch1 at 3.5 GHz with reduced Substrate length</p>	<p>Reduced Ground with reduced Substrate length</p>		<p>Res. Freq $f_r = 3.86$ GHz</p> <p>BW (GHz) (Nil)</p> <p>Bidirectional Radiation Pattern</p> <p>Gain at 3.5 GHz is 4.73 dBi</p> <p>Antenna size Miniaturization (12.676%)</p>
<p>Step-4</p> <p>$W_S = 3h + W_P + 3h = 35.686$</p> <p>$L_S = L_F + L_P + h - 1.4 = 31.688$</p> <p>$h = 1.6$</p> <p>Ground</p> <p>$W_G = W_S = 35.686$</p> <p>$L_G = L_S = 8.2$</p>	<p>Modified Patch = Feed + Patch1 @ 3.5 GHz - Patch2 @ 3.7 GHz + Patch3 @ 4.5 GHz</p>	<p>Reduced Ground with reduced Substrate length</p>		<p>Res. Freq $f_r = 4.40$ GHz</p> <p>BW (GHz) (3.54–4.94)</p> <p>Bidirectional Radiation Pattern</p> <p>Gain at 3.5 GHz is 4.95 dBi</p>

Table 2 (continued)

Step and antenna size (mm)	Patch (Front View)	Ground (Rear View)	Reflection Coefficient Characteristics (S_{11}) Plot	Antenna parameters
<p>Step-5</p> $W_S = 3h + W_P + 3h = 35.686$ $L_S = L_F + L_P + h - 1.4 = 31.688$ $h = 1.6$ Ground $W_G = W_S = 35.686$ $L_G = L_S = 8.2$	<p>Modified Patch = 1.463 mm Swapped Patch3 @ 4.5 GHz</p>	<p>Reduced Ground with reduced Substrate length</p>		<p>Res. Freq $f_r = 4.50$ GHz BW (GHz) (3.58–5.50) Bidirectional Radiation Pattern Gain at 3.5 GHz is 4.14 dBi (n79 band achieved)</p>
<p>Step-6</p> $W_S = 3h + W_P + 3h = 35.686$ $L_S = L_F + L_P + h - 1.4 = 31.688$ $h = 1.6$ Ground $W_G = W_S = 35.686$ $L_G = L_S = 8.2$	<p>Modified Patch = Mutual coupling between patch3 and (patch1-patch2)</p>	<p>Reduced Ground with reduced Substrate length</p>		<p>Res. Freq. $f_r = 3.30/3.88/4.84$ GHz BW (GHz) (3.17–5.42) Bidirectional Radiation Pattern Gain at 3.5 GHz is 4.70 dBi (n77, n78, and n79 band achieved)</p>

Table 2 (continued)

Step and antenna size (mm)	Patch (Front View)	Ground (Rear View)	Reflection Coefficient Characteristics (S_{11} Plot)	Antenna parameters
<p>Step-7</p> <p>$W_S = 3h + W_P + 3h = 35.686$</p> <p>$L_S = L_F + L_P + h - 1.4 = 31.688$</p> <p>$h = 1.6$</p> <p>Ground</p> <p>$W_G = W_S = 35.686$</p> <p>$L_G = L_S = 8.2$</p>	<p>Modified Patch =</p> <p>Mutual coupling between patch3 and (patch1-patch2)</p>	<p>Reduced Ground</p> <p>parasiti-cally Loaded with SRR</p>		<p>Res. Freq, $f_r = 3.24/4.02$ GHz</p> <p>BW (GHz) (3.13–5.06)</p> <p>Bidirectional Radiation Pattern</p> <p>Gain at 3.5 GHz is 5.14 dBi (n77, n78, and n79 bands achieved)</p> <p>With Gain Enhancement</p>

1. Metamaterial SRR Design and Effective Parameters of SRR

The metamaterial split ring resonator antenna SRR is designed in such a way that it resonates at a frequency of 3.5 GHz. The outer radius of the ring is 4.797 mm with the width and gap between rings equal to 1.0mm [3, 5]. The designed SRR will work as a parallel resonating circuit and it gives a resonating frequency of 3.5 GHz with an equivalent capacitor of 0.18pF and an inductor value is 11.5137nH. The simulated metamaterial SRR S-parameters magnitudes and phases are shown in Fig. 4a and b. The changes in reflection coefficients magnitudes and phases are observed at a frequency of 3.34 GHz. Since both the SRR and Complementary SRR (CSRR) have the same design equations for resonating frequencies. The SRR and CSRR are differentiated/identified by their permeability/permittivity values. If metamaterial has negative permittivity ($\text{Re}(\epsilon_{\text{eff}})$) values (ENG) then it behaves as SRR whereas when the permeability ($\text{Re}(\mu_{\text{eff}})$) is negative (MNG) then the metamaterial falls into the category of CSRR [9]. If both the values are found negative then the metamaterial is said to be double negative (DNG). The permittivity and permeability plots of the metamaterial SRR are shown in Fig. 4c and d. It is observed that the permittivity plot is negative and the permeability plot is positive at the resonating frequency. This guarantees that the metamaterial will properly behave like an SRR. The refractive index plot of the SRR is represented in Fig. 4e. The effective permittivity, effective permeability, and effective refractive index of the SRR are evaluated using the standard equations [5, 12, and 13].

2. Reduced Ground and SRR Parasitic Loading

Initially, the radiating patch of the antenna has ground over the entire bottom surface. It suffers with higher reflections and narrow -10 dB bandwidth from 4.98 GHz to 5.06 GHz. This has radiation patterns main lobe in the perpendicular direction of the radiating patch and a negligible minor lobe on the ground side. Consequently, the antenna has a unidirectional radiation pattern. Then ground is reduced in length towards the feed side. This will result in a wider bandwidth from 3.17 GHz to 5.42 GHz and a bidirectional radiation pattern with a gain of 4.70 dBi. This wider bandwidth not only covers n77, n78, and n79 but also covers some other 5G bands, which causes interference with the main bands. Therefore, it is essential to control the bandwidth within the limit that can cover only n77, n78, and n79 bands of Sub-6 GHz Applications. To achieve this the extra bandwidth can be eliminated by introducing either SRR or CSRR without disturbing the antenna gain and other parameters [5]. The parasitic loading of ground with single unit SRR reduces the bandwidth from 3.13 GHz to 5.06 GHz and maintains a gain of more than 5 dBi. The effect of ground length reduction and SRR parasitic loading in the ground on the reflection coefficient are illustrated in Fig. 5 and showcased in Table 3.

3. Parametric Effect of Current Mutual Coupling

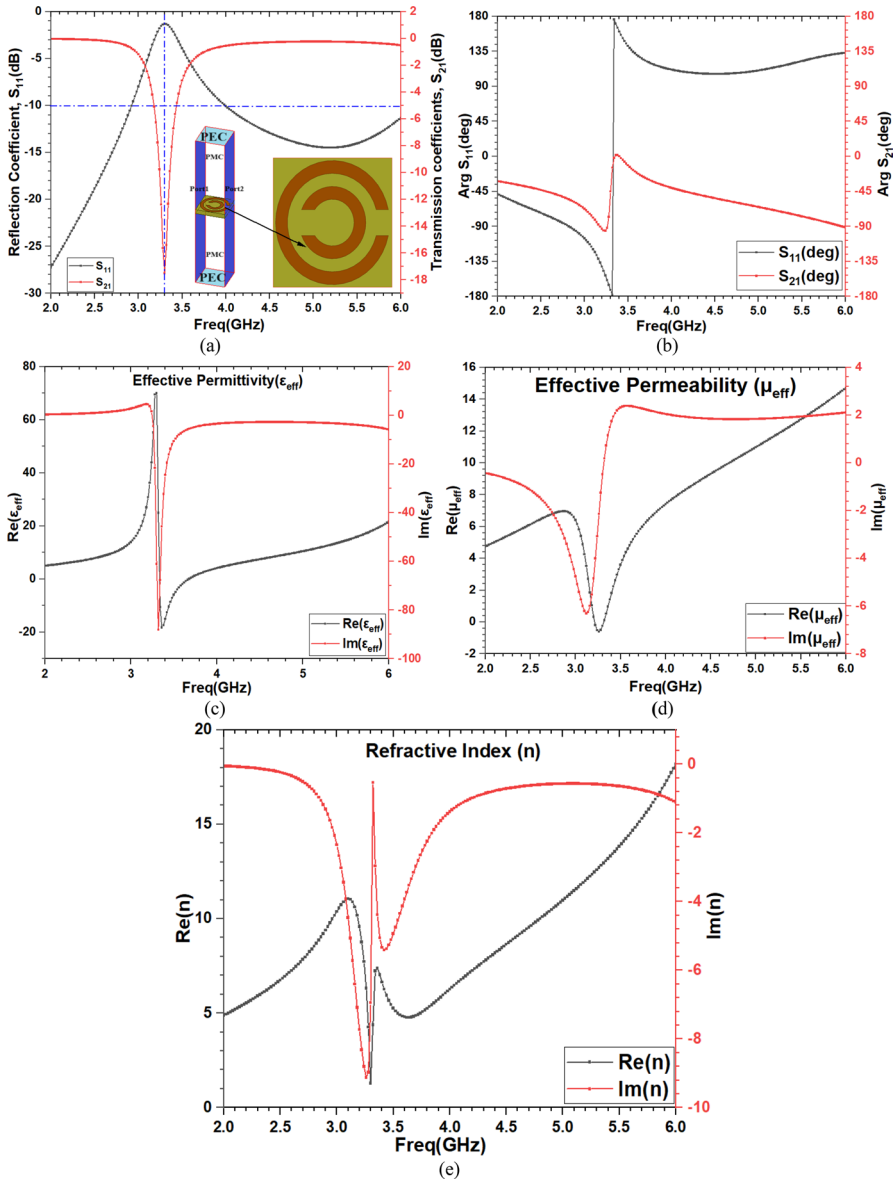


Fig. 4 Performance parameters of SRR **a** Magnitude (in dB) of S-parameters, **b** Phases (in dB) of S-parameters, **c** Permittivity Plot, **d** Permeability Plot, and **e** Refractive Index plot

The current coupling between the patch and U-shaped stub is dependent upon the three parameters namely the distance between the coupling arm and U-shaped stub, also on the length ($L_{coup.}$) and width ($W_{coup.}$) of the coupling arm. The length of the coupling arm and the mutual coupling distance (M_{123}) are correlated to each other the variation in one automatically changes the other parameter. The parametric effect of

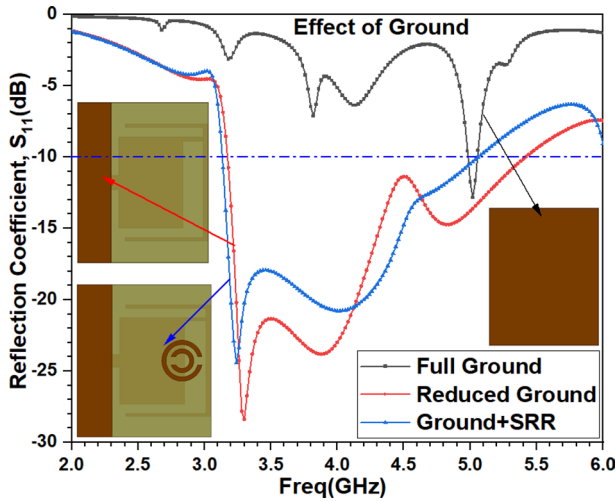


Fig. 5 Effect of modifications in Ground

Table 3 Effect of ground

Ground	Resonant frequency (GHz)	Reflection coefficient S_{11} (dB)	Bandwidth (GHz)	Gain (dBi)
Full ground	5.02	-12.86	4.98–5.06	5.33 (unidirectional)
Reduced ground	3.30, 3.88, 4.82	-28.38, -23.81, -14.74	3.17–5.42	4.70 (bidirectional)
Reduced ground with SRR	3.24, 4.0	-20.94, -20.79	3.13–5.06	5.14 (bidirectional)

the variation in coupling distance coupling length and coupling with are showcased in Table 4 And their effect on the reflection coefficient is displayed in Fig. 6a and b. The mutual coupling distance (M_{123}) or coupling length of the arm Is varied in a step size of 0.153 mm while keeping the coupling width of the arm constant and equal to 0.8 mm. This parametric change in the coupling distance effect on the reflection coefficient is shown in Fig. 6a. On the other hand, when the coupling width of the arm Is varied in a step size of 0.2 mm while keeping the coupling distance constant equal to 0.153 mm. This parametric change effect on the reflection coefficient is shown in Fig. 6b.

Table 4 Parametric Effect of Mutual Coupling

Parametric	Mutual coupling (in mm)	Resonant frequency (GHz)	Reflection coefficient S_{11} (dB)	Bandwidth (GHz)	Peak current magnitude (A/m)	Gain (dBi)
Mutual coupling distance (M_{123}) or Coupling length (L_{coup})	$W_{coup} = 0.8$ (fixed) $L_{coup} = 4.8 + 0.153$ $= 4.953$ $M_{123} = 0$	3.36, 4.24	- 11.49, - 18.01	3.33-3.40, 3.62-5.09	Total current = 39.6785 Coupling current = 19.86 (50%)	4.61
	$W_{coup} = 0.8$ (fixed) $L_{coup} = 4.8$ $M_{123} = 0.153$	3.24, 4.0	- 20.94, - 20.79	3.13-5.06	Total current = 65.31 Coupling current = 39.3(60.018%)	5.14
	$W_{coup} = 0.8$ (fixed) $L_{coup} = 4.8 - 0.153$ $= 4.647$ $M_{123} = 2 * 0.153 = 0.306$	3.26, 3.96	- 26.57, - 24.28	3.15-5.06	Total current = 49.3393 Coupling current = 14.87 (30.13%)	5.18
	$W_{coup} = 0.8$ (fixed) $L_{coup} = 4.8 - 2 * 0.153 = 4.494$ $M_{123} = 3 * 0.153 = 0.459$	3.34	- 37.26	3.21-5.13	Total current = 66.13 Coupling current = 26.85 (40.60%)	5.17
	$W_{coup} = 0.8$ $L_{coup} = 4.8$ (fixed) $M_{123} = 0.153$ (fixed)	3.24, 4.0	- 20.94, - 20.79	3.13-5.06	Total current = 65.31 Coupling current = 39.3 (60.018%)	5.14
Mutual Coupling width (W_{coup})	$W_{coup} = 0.8 + 0.2 = 1.0$ $L_{coup} = 4.8$ (fixed) $M_{123} = 0.153$ (fixed)	4.0	- 21.82	3.14-5.08	Total current = 49.285 Coupling current = 14.92 (30.27%)	5.08
	$W_{coup} = 0.8 + 2 * 0.2 = 1.2$ $L_{coup} = 4.8$ (fixed) $M_{123} = 0.153$ (fixed)	3.81	- 20.79	3.12-4.87	Total current = 110.1625 Coupling current = 22.19 (20.14%)	5.09
	$W_{coup} = 0.8 + 3 * 0.2 = 1.4$ $L_{coup} = 4.8$ (fixed) $M_{123} = 0.153$ (fixed)	3.88	- 20.40	3.09-4.94	Total current = 37.064 Coupling current = 14.85 (40.06%)	5.08
	$W_{coup} = 0.8$ $L_{coup} = 4.8$ (fixed) $M_{123} = 0.153$ (fixed)	3.24, 4.0	- 20.94, - 20.79	3.13-5.06	Total current = 65.31 Coupling current = 39.3 (60.018%)	5.14
	$W_{coup} = 0.8 + 0.2 = 1.0$ $L_{coup} = 4.8$ (fixed) $M_{123} = 0.153$ (fixed)	4.0	- 21.82	3.14-5.08	Total current = 49.285 Coupling current = 14.92 (30.27%)	5.08

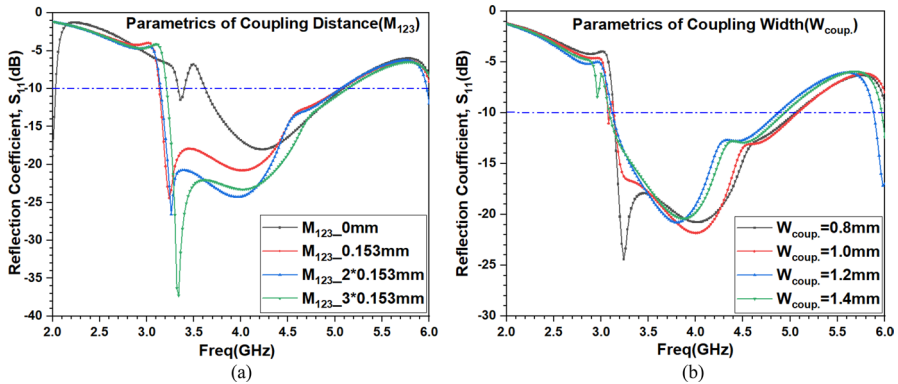


Fig. 6 Parametric of mutual coupling

3 Results and discussions

The following section deals with the antenna measurement and their validation by comparing the simulated antenna parameters. It also describes the electrical equivalent circuit of the antenna as well as the comparison of the similarly existing recently published antennas.

A. Fabricated Antenna Prototype

The proposed antenna designed using CST and HFSS software is fabricated using photolithography UV exposure and a chemical etching process. The antenna is fabricated on a piece of low-cost FR4 substrate material of thickness 1.6 mm. The fabricated antenna prototype model print view and rear view are shown in Fig. 7a and b. The reflection coefficient of the antenna is measured using the Vector Network Analyzer (VNA) and the radiation pattern and gain of

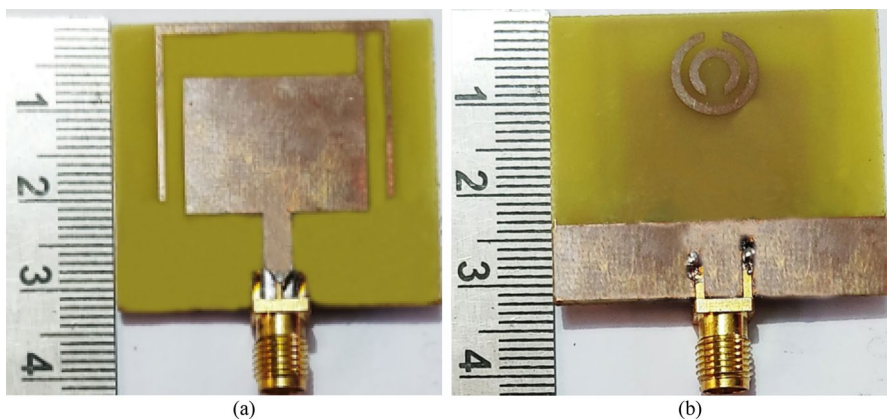


Fig. 7 Antenna prototype model **a** Front View, and **b** Rear View

the fabricated antenna are measured using the anechoic chamber. The measured reflection coefficient of the antenna is then compared with the simulated HFSS and CST software reflection coefficient for their validation. All three reflection coefficients are found in the shape agreements and these plots have nearly the same resonating frequency and -10 dB bandwidth. The shape of the measured reflection coefficient is a little distorted as compared to the simulated reflection coefficients. The possible reason for this error is either defects in the soldering of the 50Ω SMA connector or a dimensional error of the fabricated antenna. These errors also result in deviation in the resonant frequencies and their -10 dB bandwidths. The measured and simulated reflexive coefficient of the proposed antenna is shown in Fig. 8.

B. Antenna Gain and Radiation Efficiency

The comparison between simulated and measured antenna gains is presented in Fig. 9. All three gain curves exhibit similar shapes. The CST-simulated antenna achieves a peak gain of 7.2 dBi at 3.5 GHz, while the HFSS-simulated antenna peaks at 5.40 dBi. The measured antenna demonstrates a peak gain of 6.8 dBi. The shape of the HFSS-simulated antenna gain closely resembles that of the measured antenna, validating its performance.

Furthermore, the HFSS-designed simulated radiation efficiency is compared with the CST-designed simulated radiation efficiency, showing good agreement from 3.2 GHz to 5.4 GHz. The CST antenna achieves a maximum radiation efficiency of 99.55%, whereas the HFSS simulated antenna achieves 91.43% at the design frequency of 3.5 GHz. These radiation efficiency comparisons are depicted in Fig. 10.

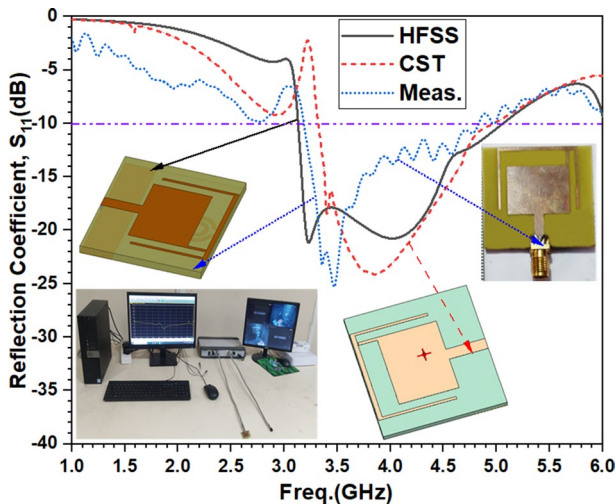


Fig. 8 Reflection coefficients

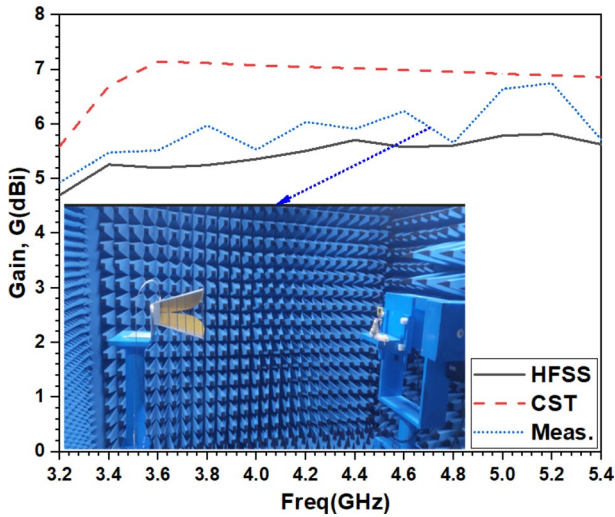


Fig. 9 Simulated and measured antenna gains

A comprehensive comparison of measured and simulated antenna performance parameters is presented in Table 5.

C. Antenna Radiation Patterns

The antenna is proposed to cover 5G Sub-6 GHz n77 (3700 MHz), n78 (3500 MHz), and n79 (4500 MHz) bands. Therefore, for the validation of the antenna radiation patterns in the E-plane and the H-plane are evaluated at their central frequencies at 3.5 GHz 3.7 GHz, and 4.5 GHz respectively in the anechoic chamber of frequency 43 GHz. The simulated and measured E-plane and H-plane radiation patterns at the central frequencies are compared and found in good agreement as illustrated in Fig. 11.

D. Current Distribution

The current coupling between the patch and the U-shaped stub is dependent on three parameters: the distance between the coupling arm and the U-shaped stub, as well as the length ($L_{\text{coup.}}$) and width ($W_{\text{coup.}}$) of the coupling arm. The length of the coupling arm and the mutual coupling distance (M_{123}) are correlated to each other; the variation in one automatically changes the other parameter. The maximum current is coupled to SRR at 3.5 GHz while the minimum current magnitude is coupled to SRR at 4.5 GHz. The magnitude of current coupling in the U-shaped stub and coupling arm decreases as the frequency increases from 3.5 GHz to 4.5 GHz. The magnitude of current density distributions of the proposed antenna at the center frequencies 3.5 GHz, 3.7 GHz, and 4.5 GHz of the n77, n78, and n79 bands are indicated in the top and bottom surfaces of the

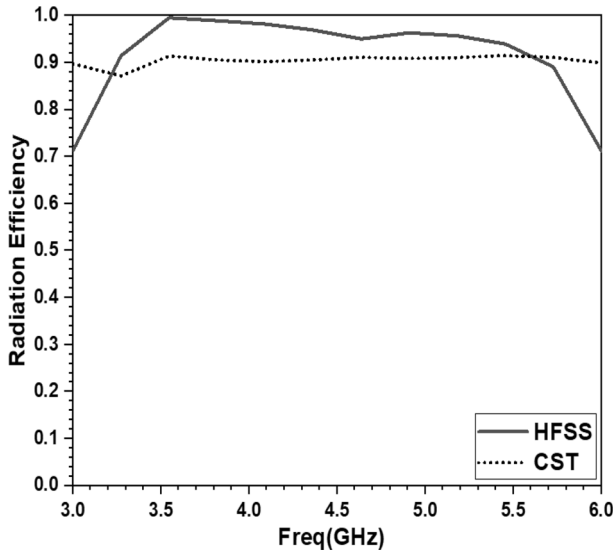


Fig.10 Antenna radiation efficiency

Table 5 Simulated and measured antenna performance parameters

Mode	f_r (GHz)	S_{11} (dB)	- 10 dB BW (GHz)	Peak Gain (dBi)	Maximum Rad. Efficiency (%)
HFSS Simulated	3.23, 4.022	-21.16, -20.77	3.13–5.06	5.71	99.55
CST Simulated	3.40, 3.84	-18.42, -24.12	3.30–5.01	7.14	91.43
VNA (MS46122B) Measured	3.355, 3.466	-23.26, -25.30	3.18–4.83	6.75	–

antenna as displayed in Fig. 12a–c respectively. The red color in Fig. 12 corresponds to the maximum magnitude while the blue color corresponds to the minimum current.

E. Electrical Equivalent Circuit

The designed S-parameter plot of the proposed antenna exhibits a single passband with two resonant frequencies at 3.24 GHz and 4.0 GHz, each displaying minimum reflection coefficient values. At these resonant frequencies, the impedance values are $(45.87-j7.60) \Omega$ and $(58.18-j5.57) \Omega$, respectively. The reactive components at these frequencies are negligible, resulting in two-series RLC resonances in parallel arms.

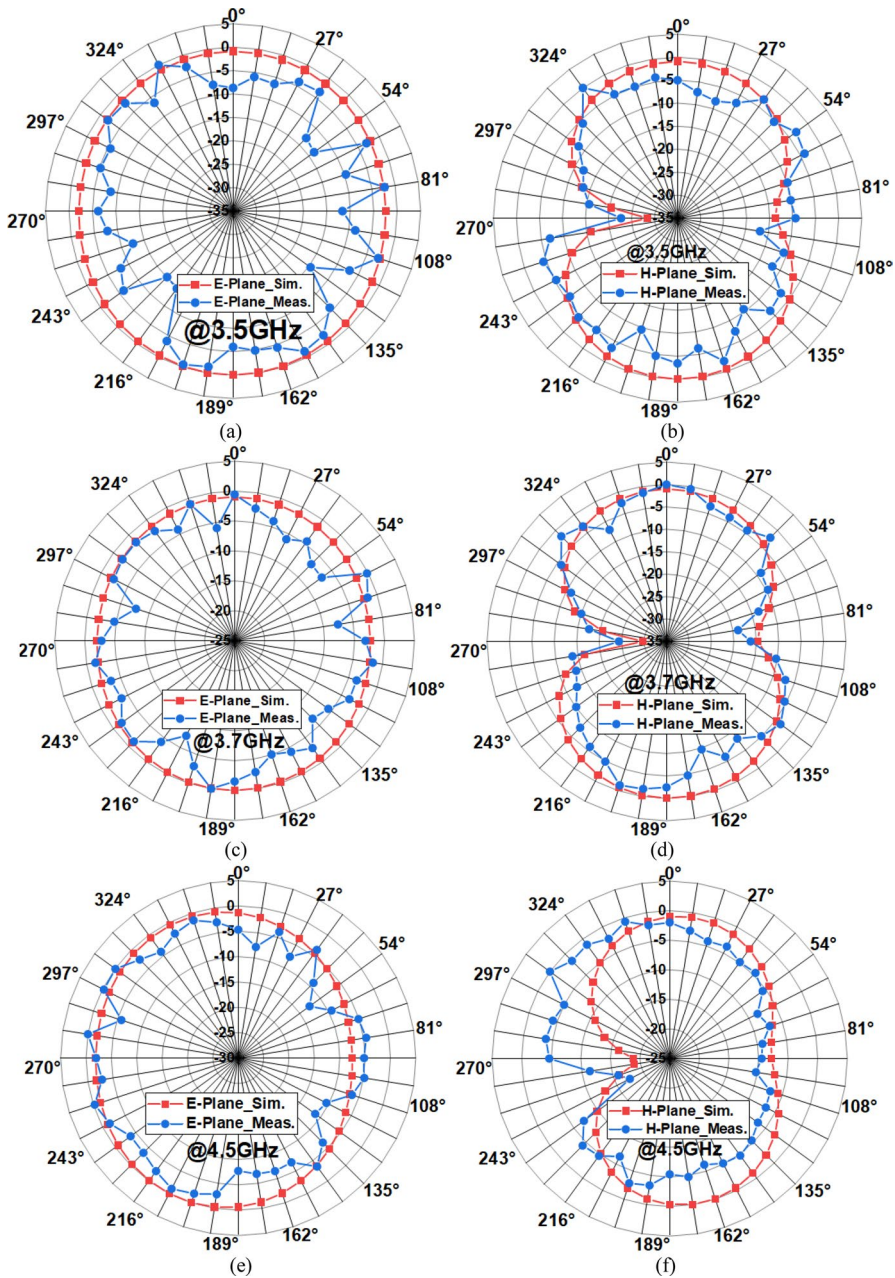


Fig. 11 Radiation patterns **a** E-Plane@3.5 GHz, **b** H-Plane@3.5 GHz **c** E-Plane@3.7 GHz, **d** H-Plane@3.7 GHz, **e** E-Plane@4.5 GHz, and **f** H-Plane@4.5 GHz

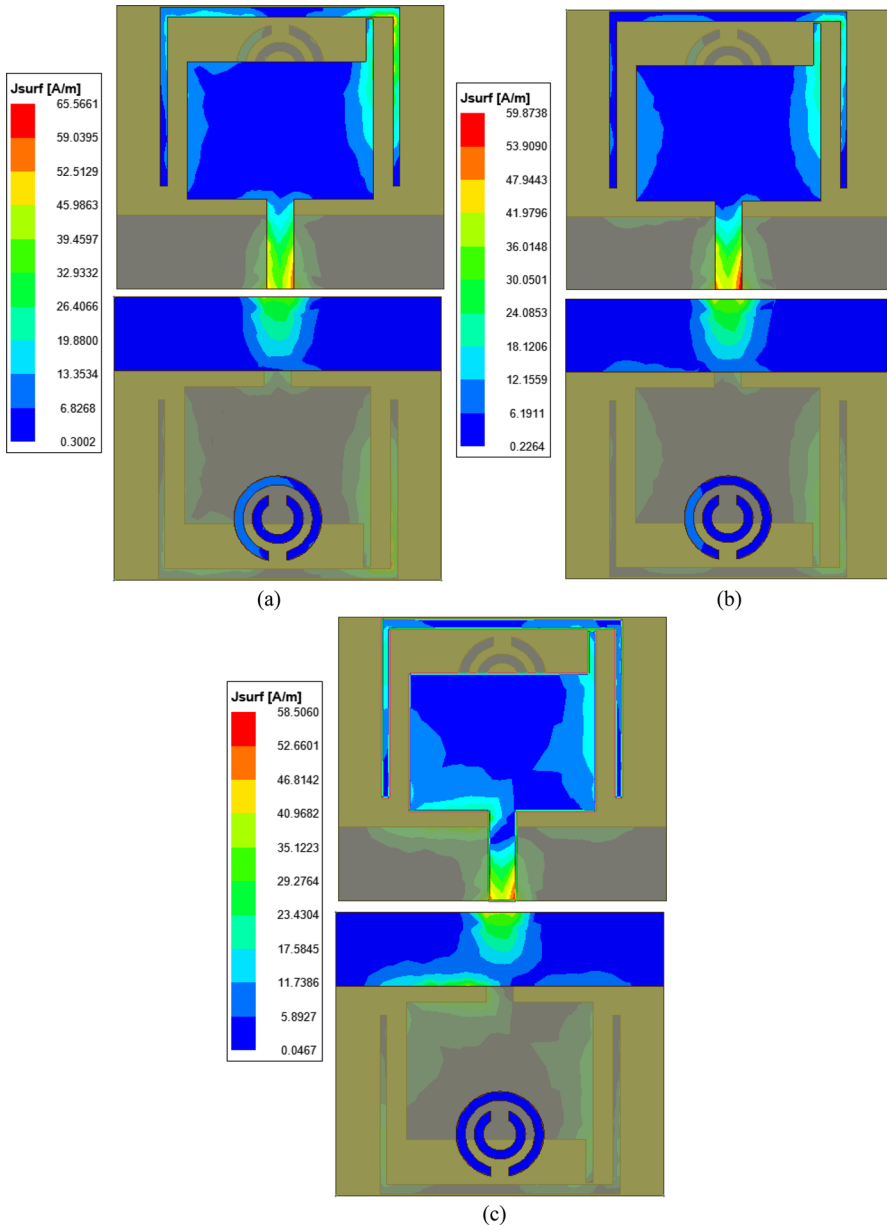


Fig. 12 Magnitude of Current densities distributions **a** at 3.5 GHz, **b** at 3.7 GHz, and **c** at 4.5 GHz

A 50Ω termination serves as the source, with frequency ranging from 2 to 6 GHz in 0.02 GHz increments. Initially, the overall equivalent circuit parameters (R , L , and C) underwent assessment using general series and parallel RLC resonance circuit analysis. These parameters were further refined using ADS

software for validation. The specific RLC parameter values, both evaluated and fine-tuned, are elaborated in Table 6.

The equivalent circuit of the proposed antenna is illustrated in Fig. 13, while Fig. 14 presents a comparison of the reflection coefficient (S_{11}) plots. These plots exhibit excellent alignment at the resonance frequencies..

F. State-of-the-Art of the Proposed Antenna

The comparative analysis of the proposed antenna with recent literature is presented in Table 7. This work is observed to result in miniaturization, improved radiation efficiency, and gain at the intended frequency.

An 85.33% miniaturized antenna proposed in reference [1], is specific to only the n78 band and has a lower gain of 2.92 dBi [1]. The antenna presented in reference [14], has a maximum gain of 7.95 dBi with narrow bandwidth from 3.40 to 3.60 GHz. Therefore, it is partially suitable for the n78 band only [14]. The antenna proposed in reference [11], has a maximum gain of 8.4 dBi with wide bandwidth from 3.12 to 3.90 GHz. Therefore, it is suitable for the n78 band only [11]. An antenna described in reference [2], is specific to only 5G n78 band and has a peak gain of 8.2 dBi [1]. The antenna published in reference [20], is a compact 2×2 MIMO antenna, that covers 5G sub-6 GHz n77, n78, n79, wi-fi5, and wi-fi6 with lower gain and wide bandwidth [20]. In these published antennas either gain is higher or narrower bandwidth [2, 6, 11, 14] or wider bandwidth with lower antenna gains [1, 7]. Therefore, it is challenging to achieve wider bandwidth and higher gain or maintain the antenna gain above 5 dBi. The interference reduction with wider bandwidth is also one more challenging aspect. The bandwidth control and maintaining gain above 5dBi with reduced interference with other applications like Wi-Fi5 and Wi-Fi6 is achieved by introducing a metamaterial (MTM) split ring resonator (SRR). The parasitic loading of SRR in the proposed work maintains the gain of the antenna above the 5 dBi and eliminates the extra bandwidth by proper placing of the SRR in the ground surface of the antenna [5].

The accuracy of the design is validated by the measurement results. The proposed design is compared with related works in the literature. It is clear that the proposed miniaturization technique provides considerable gain and covers important most popular Sub-6 GHz bands.

4 Conclusion

The low-cost designed antenna performance parameters have been analyzed and improved by parasitic loading of U-stubs, SRR, and current mutual coupling arms between the patch and U-stubs. The extra bandwidth and gain of the antenna are controlled by parasitic loading of the antenna ground with metamaterial SRR. The parasitic loading of SRR improves the gain and reduces the -10 dB bandwidth. The Sub-6 GHz (FR1 frequency range of 5G) fabricated and designed antenna

Table 6 Equivalent circuit RLC component values

Resonance frequency	R(Ω) (Manual)	R(Ω) ADS tuned	L (nH) (Manual)	L (nH) ADS tuned	C(pF) (Manual)	C(pF) ADS tuned
$f_{r1} = 3.24$ GHz	59.89	47.912	4.94	9.1086	0.49	0.3087
$f_{r2} = 4.0$ GHz	59.89	61.0878	4.93	4.4595	0.32	0.2816

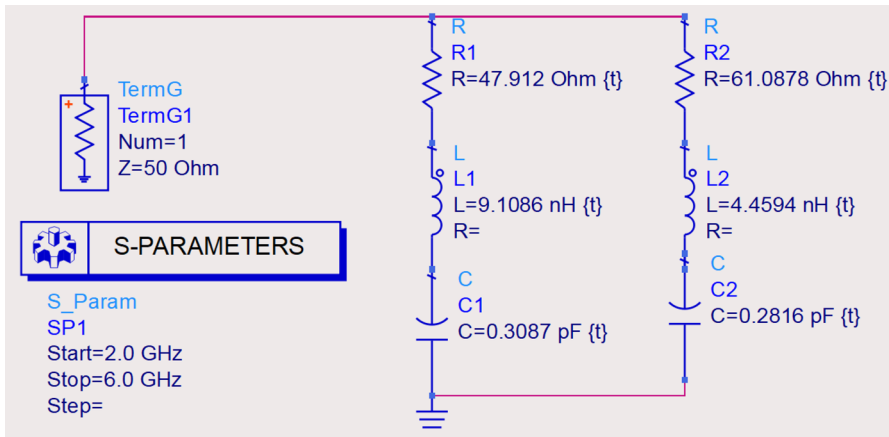


Fig. 13 RLC electrical equivalent circuit of the proposed antenna

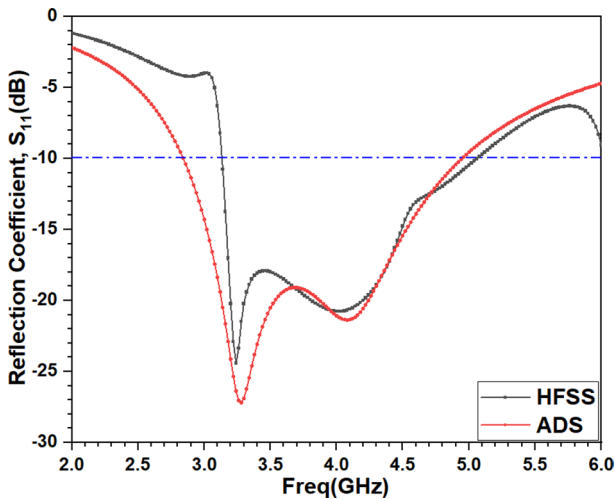


Fig. 14 RLC circuit reflection coefficients validation

performance parameters in terms of their reflection coefficients, -10 dB BW, radiation Patterns, gain, efficiency, and current distributions are compared and they found in excellent agreement that validate the antenna. The manually generated electrical equivalent RLC circuit of the antenna is validated using the ADS software. The proposed antenna is a therefore suitable choice for the 5G FR1 frequency bands n77 (3.3–4.2 GHz), n78 (3.3–3.8 GHz), n79 (4.4–5.0 GHz), and additionally suitable for

Table 7 Comparison of the proposed antenna with existing similar antennas

Ref./Year	Design Freq. (GHz)	Sub. used	Antenna size (L × W × h)	−10 dB BW (GHz)	Rad. Eff. (%)	Gain (dBi)	Ant. Size Reduction (%)	Parasitic load	RLC equ. circuit	Sub-6 GHz bands coverage
[11] 2022	3.5	FR4	$0.151\lambda_0 \times 0.303\lambda_0 \times 0.018\lambda_0$	3.18–4.06	95.37	2.92	85.33	Not	Not given	n78 only
[2] 2020	2.5	FR4	$0.29\lambda_0 \times 0.30\lambda_0 \times 0.22\lambda_0$	3.15–3.67	NA	8.2	Not done	Not	Not given	n78 band only
[6] 2023	3.6	FR4	$0.141\lambda_0 \times 0.28\lambda_0 \times 0.018\lambda_0$	3.3–3.9	92.82	4.35	86.74	Stub	given	n78 only
[7] 2023	3.12	FR4	$0.258\lambda_0 \times 0.31\lambda_0 \times 0.0186\lambda_0$	3.12–7.12	95	2.6	Not done	Not	Not given	n77, n78, and n79, Wi-Fi5 and Wi-Fi6
[11] 2019	3.5	F4B $\epsilon_r = 2.65$ $h = 0.8$ mm	$0.758\lambda_0 \times 0.758\lambda_0 \times 0.0093\lambda_0$	3.12–3.9	NA	8.4	Not done	Not	Not given	n78 band only
[14] 2020	3.5	FR4	$0.35\lambda_0 \times 0.525\lambda_0 \times 0.018\lambda_0$	3.4–3.6	88.40	7.95	Not done	Not	Not given	Partial n78 band only
[19] 2021	3.0	RT Rogers 4330 h $\epsilon_r = 2.65$ $= 0.8$ mm	$0.228\lambda_0 \times 0.338\lambda_0 \times 0.008\lambda_0$	3.42–4.25	91.38	4.1	Not done	SRR	Not given	n77 and n78 band only
This work	3.5	FR4	$0.416\lambda_0 \times 0.423\lambda_0 \times 0.0186\lambda_0$	3.13–5.06	99.55	5.14	12.676	U-stub and SRR	given	n77, n78, and n79

other bands n48 (3550–3700 MHz), Wi-MAX(3.5 GHz), Wi-Fi/WLAN (3.6 GHz, 4.9 GHz, 5 GHz) applications. In the future, the antenna can be converted into 2×2 or 4×4 MIMO/Array structures easily. Moreover, the antenna can easily be frequency reconfig.d by introducing an RF PIN diode (BAR 64-02 V) between the coupling arm and U-stubs. The measured results agreement confirm its suitability for low-power compact electronic gadgets.

Author Contributions Sudharani Chidurala was primarily responsible for the conceptualization and design of the antenna. She also contributed significantly to the analysis and interpretation of the results, as well as to the writing and editing of the manuscript. Prakasa Rao Amara contributed to the drafting and revision of manuscript.

Funding There is no funding received for this study.

Data Availability No datasets were generated or analysed during the current study.

Declarations

Conflict of interest The authors declare that they have no conflict of interest.

References

1. Varshney, A., Sharma, V., Neebha, T. M., & Kumar, R. (2022). *A compact low-cost impedance transformer-fed wideband monopole antenna for Wi-MAX N78-band and wireless applications* (pp. 315–328). CRC Press.
2. Chen, Y., Liu, Q., Zhang, Y., Li, H., and Zong, W. (2020) Design of a compact base station antenna for 5G N78-band application. *IEEE 3rd International Conference on Electronic Information and Communication Technology (ICEICT)*, 229–231. <https://doi.org/10.1109/ICEICT51264.2020.9334286>.
3. Varshney, A., Cholake, N., & Sharma, V. (2021). Low-cost ELC-UWB fan-shaped antenna using parasitic SRR triplet for ISM band and PCS applications. *International Journal of Electronics Letters*, 10(4), 391–402.
4. Varshney, A., Neebha, T. M., Sharma, V., Jency, J. G., & Andrushia, A. D. (2022). Dodecagon-shaped frequency reconfigurable antenna practically loaded with 3-delta structures for ISM band and wireless applications. *IETE Journal of Research*, 69(1), 1–13.
5. Varshney, A., Sharma, V., Neebha, T. M., & Kumari, N. P. (2023). Notch-band eliminator wideband CSRR loaded monopole fractal antenna for ISM and PCS communications. *World Journal of Engineering*. <https://doi.org/10.1108/WJE-08-2022-0333>
6. Varshney, A., Sharma, V., & Sharma, A. K. (2023). RLC-equivalent Circuit-based Stub Loaded 2×2 MIMO Antenna for X-band applications. *Microwave Review*, 29(1), 44–54.
7. Addepalli, T. (2023). Compact MIMO Diversity Antenna for 5G Sub: 6 GHz (N77/N78 and N79) and WLAN (Wi-Fi 5 and Wi-Fi 6) Band Applications. *Wireless Personal Communications*, 132, 2203–2223. <https://doi.org/10.1007/s11277-023-10718-4>
8. Jain, P., Thourwal, A., Sardana, N., Kumar, S., Gupta, N. and Singh, A. K. I-shaped metamaterial antenna for X-band applications. Progress In *Electromagnetics Research Symposium - Spring (PIERS)*, St. Petersburg, Russia, 2017: 2800–2803. <https://doi.org/10.1109/PIERS.2017.8262229>.
9. Saleh, A. A., & Abdullah, A. S. (2014). A novel design of patch antenna loaded with complementary split-ring resonator and L- L-shape slot for (WiMAX/WLAN) applications. *IJWMT*, 4(3), 16–25. <https://doi.org/10.5815/ijwmt.2014.03.02>

10. Singh, S., Sethi, G., & Khinda, J. S. (2023). Low-loss UWB mm-wave monopole antenna using patch size enhancement for next-generation (5G and Beyond) communications. *Journal of Infrared, Millimeter, and Terahertz Waves*, *44*(11), 936–963.
11. Li, Y., Zhao, Z., Tang, Z., & Yin, Y. (2019). Differentially-fed, wideband dual-polarized filtering antenna with novel feeding structure for 5G sub-6 GHz base station applications. *IEEE Access*, *7*, 184718–184725. <https://doi.org/10.1109/ACCESS.2019.2960885>
12. Islam, S. S., Rashed, M., Faruque, I., & Islam, M. T. (2015). A new direct retrieval method of refractive index for the metamaterial. *Current Science*, *109*(2), 337–342.
13. Hossain, M. B., Faruque, M. R. I., Islam, S. S., et al. (2021). Modified double dumbbell-shaped splitting resonator-based negative permittivity metamaterial for satellite communications with a high effective medium ratio. *Scientific Report*, *11*, 19331. <https://doi.org/10.1038/s41598-021-98703-4>
14. Sahoo, A. B., Patnaik, N., Ravi, A., Behera, S., and Mangaraj, B. B. (2020) Design of a miniaturized circular microstrip patch antenna for 5G applications, *International Conference on Emerging Trends in Information Technology and Engineering (ic-ETITE)*,: 1–4. <https://doi.org/10.1109/ic-ETITE47903.2020.374>.
15. Varshney, A., Sharma, V., Nayak, C., Goyal, A. K., & Massoud, Y. (2023). A low-loss impedance transformer-less fish-tail-shaped MS-to-WG transition for K-/Ka-/Q-/U-band applications. *Electronics*, *12*, 670. <https://doi.org/10.3390/electronics12030670>
16. Ouyang, Y., & Chappell, W. J. (2008). High-frequency properties of electro textiles for wearable antenna applications. *IEEE Transactions on Antennas Propagation*, *56*(2), 381–389.
17. Purohit, S., & Raval, F. (2014). Wearable -textile patch antenna using jeans as substrate at 2.45 GHz. *International Journal of Engineering Research & Technology (IJERT)*, *3*(5), 2456–2460.
18. Yang, L., Martin, L., Staiculescu, D., Wong, C., & Tentzeris, M. (2008). Conformal magnetic composite RFID for wearable RF and bio-monitoring applications. *IEEE Transactions on Microwave Theory and Techniques*, *56*(12), 3223–3230.
19. Sharma, R., & Khanna Geetanjali, R. (2022). Compact sub-6 GHz and mmwave 5G wideband 2×1 MIMO antenna with high isolation using parasitically placed double negative (DNG) isolator. *Wireless Personal Communications*, *122*, 2839–2857. <https://doi.org/10.1007/s11277-021-09032-8>
20. Varshney, A., Sharma, V., Elfergani, I., Zebiri, C., Vujicic, Z., & Rodriguez, J. (2022). An inline V-Band WR-15 transition using antipodal dipole antenna as RF energy launcher@ 60 GHz for satellite applications. *Electronics*, *11*(23), 3860.

Publisher's Note Springer Nature remains neutral with regard to jurisdictional claims in published maps and institutional affiliations.

Springer Nature or its licensor (e.g. a society or other partner) holds exclusive rights to this article under a publishing agreement with the author(s) or other rightsholder(s); author self-archiving of the accepted manuscript version of this article is solely governed by the terms of such publishing agreement and applicable law.